Supplementary Material

Solketal Production Using an Eco-Friendly reduced Graphene oxide as catalyst

Figure S1. Batch reactor used in all ketalization reactions (Parr Instruments Inc. - Model 4848B), made of stainless steel, with a useful volume of 100 mL, in a simple batch system, with a maximum working pressure of 200 bar. This reactor has a temperature and pressure controller. Also controlled agitation and external blanket for heating.

Table S1. Estimated values for the distance between layers, average crystallite size, and number of layers for GFT_H, rGO_H, GFT_E and rGO_E materials

Materials	2θ (⁰)	d_{001} (nm)	L_{002} (nm)	N[1]
GFT_H	36.32	0.3385	15.00	44
rGO_H	26.21	0.3399	5.00	17
GFT_E	26.51	0.3360	31.00	91
rGO_E	29.29	0.3387	5.00	15

[1] Number of layers.

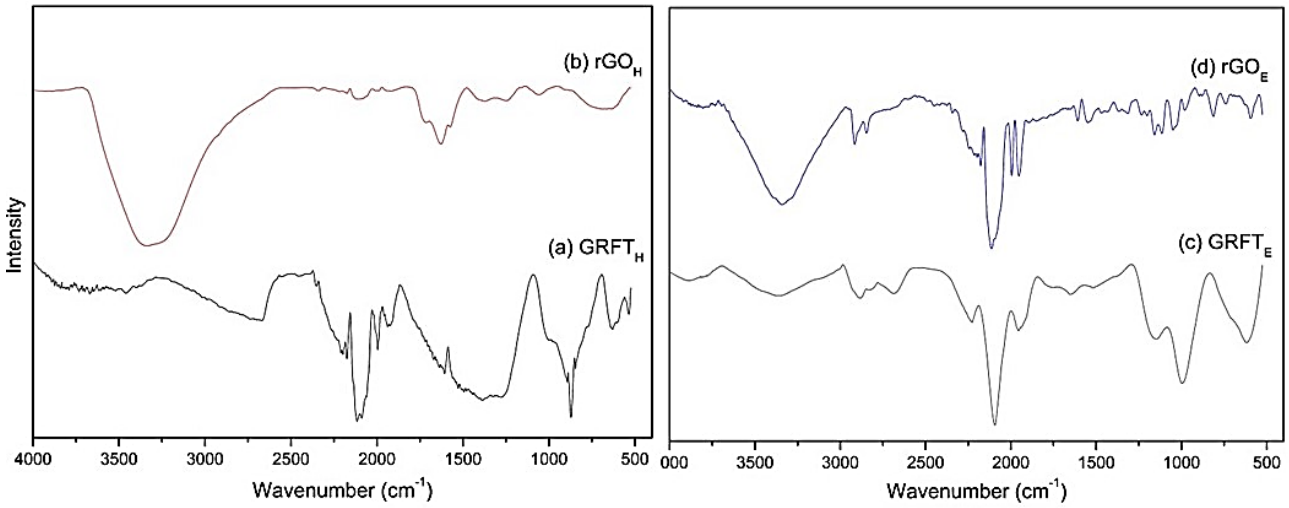

Figure S2. Infrared spectra of graphite flakes (a) GRFH and reduced graphene oxide, (b) rGOH, obtained by the Hummers method; carpenter's pencil graphite (c) GFTE and reduced graphene oxide, (d) rGOE, obtained by the electrochemical method from carpenter's pencil graphite.

Table S2 . Assignments of the main bands in the infrared spectra for the GFTH, rGOH, GFTE and rGOE materials.[1–10]

GFT$_E$	rGO$_E$	GFT$_E$	rGO$_E$	Assignments of the main bands
3488	3338	3369	3360	Stretching vibrations of -OH bonds. These bands can also be attributed to -COOH and C-OH bonds.
-	-	2887 2831	2913 2842	Stretching vibrations of C-H bonds in CH_3 and CH_2 groups.
2117	2103	2096	2111 2086	Conjugated C=C-C or C=C=O bonds of graphene layers and reduced graphene oxide, respectively. Or CO_2.
1996	1925	1950	2000 1950	C-H bond in aromatic compounds.
1612	1638	1650	1612	C=C bonds associated with the vibrations of non-oxidized graphite, predominantly composed of sp^2 hybridized carbon atoms.
-	-	1643	1600	Vibrations of conjugated C=C bonds in aromatic compounds.
-	1578	-	1538	Vibrations of the carbonyl group (-C=O) bonds in rGO and vibrations of the epoxy groups.
1409	-	-	1444	Stretching vibrations of the carboxyl group (-COOH).
-	1388	-	1365	Vibration of the -OH bond in alcohols.
-	1247	-	1234	C-OH bonds in reduced graphene oxide (rGO).
-	-	1158	1204 1158	C-O bond in alcohols and phenols.
-	-	-	1121	C6-OH bond of the primary alcohol group, phenols.
-	1076	-	1051	Stretching vibration of C-O-C bonds in the epoxy group.

-	-	995	980	Vibration of C=C bonds.
869	897	-	894	Vibration of aromatic ring bonds.
-	-	797	815	Vibration of C-H bonds.
634	631	614	590	Vibration of bonds in structures derived from benzene..

Table S3. Acidity results obtained through acid-base titration for the materials tested as catalysts.

Material	Acidity (mmol H^+ g^{-1})
rGO_H	0.24 ± 0.02
rGO_E	0.22 ± 0.02

Table S4. Acidity results for the catalysts obtained by acid-base titration before and after five reactions.

Material	Acidity (mmol de H^+ g^{-1})
rGO_H Before	0.24 ± 0.02
rGO_H After	0.08 ± 0.02
rGO_E Before	0.22 ± 0.02
rGO_E After	0.11 ± 0.03

Pseudo-Homogeneous Kinetic Model Evaluation

The first approach utilized a pseudo-homogeneous kinetic model, providing information about the direction the reaction equilibrium tends (toward products or reactants). This model considers the reaction as bimolecular and reversible:

$$A + B \leftrightarrow C + D \quad \text{(Equation S1)}$$

A = glycerol; B = acetone; C = solketal, and D = water. To simplify the model, dioxan was disregarded in this study since dioxan is an isomer of solketal and wouldn't introduce differences in the molar balance of the process.

And its rate is given by:

$$(-r_A) = C_{A_0}\frac{dX_A}{dt} = k_1 C_A C_B - k_2 C_C C_D \quad \text{(Equation S2)}$$

Where ($-r_A$) is the rate of glycerol consumption; C_{A0} = initial concentration of glycerol (mol L^{-1}); X_A = glycerol conversion; C_A = final concentration of glycerol (mol L^{-1}) at time t (min); C_A = final concentration of glycerol (mol L^{-1}) at time t (min); C_B = final concentration of acetone (mol L^{-1}) at time t (min); C_C = final concentration of solketal (mol L^{-1}) at time t (min); C_D = final concentration of glycerol (mol L^{-1}) at time t (min); k_1 = rate constant of the forward reaction, and k_2 = rate constant of the reverse reaction.

Furthermore, considering that:

$$C_A = C_{A_0}(1 - X_A) \quad \text{(Equation S3)}$$
$$C_B = C_{A_0}(M - X_A) \quad \text{(Equation S4)}$$
$$C_C = C_{A_0}X_A \quad \text{(Equation S5)}$$
$$C_D = C_{A_0}X_A \quad \text{(Equation S6)}$$

With $M=C_{B0}/C_{A0}$, where C_{A0} = 1.57 mol L^{-1} and C_{B0} = 6.06 mol L^{-1}.

For the calculation of the equilibrium constant or thermodynamic equilibrium constant (K), the following expression was used:

$$K = \frac{C_C C_D}{C_A C_B} = \frac{k_1}{k_2} \quad \text{(Equation S7)}$$

When $C_{B0} > C_{A0}$, the equilibrium results in:

$$K = \frac{\left(X_{A_{eq}}\right)^2}{\left(1-X_{A_{eq}}\right)-\left(M-X_{A_{eq}}\right)} \quad \text{(Equation S8)}$$

Isolating $X_{A_{eq}}$:

$$X_{A_{eq}} = \frac{KM+K-\sqrt{K^2M^2-2K^2M+K^2+4KM}}{K-1} \quad \text{(Equation S9)}$$

To validate the model, the method chosen was the Minimization of the Sum of Squared Residuals (Q). The goal is to minimize the total sum of squared residuals across all experimental data points. This involves finding the parameter values of the model that minimize this sum. [11,12]

$$\mathrm{Q} = \sum_{i=1} n \left(X_{A_{CAL}} - X_{A_{EXP}}\right)^2 \quad \text{(Equation S10)}$$

Several approaches to finding these parameter values minimize the sum of squared residuals. A typical system is the method of least squares, which entails analytically minimizing the sum of the squares of the residuals. [11,12]

Heterogeneous Kinetic Model Evaluation

The kinetic study in heterogeneous catalysis is based on seven steps: [13,14]

1. Diffusion of reactants from the bulk fluid to the external surface of the catalyst (external diffusion);
2. Diffusion of reactants from the external surface of the catalyst into the pores (internal diffusion); this step involves the approach of reactants to the active sites of the catalyst for adsorption;
3. Chemical or physical adsorption of the reactants. Depending on the nature of the molecular forces between the adsorbent and the adsorbate, either chemical or physical adsorption occurs. If the binding forces are weak and there is no modification in the chemical nature of the adsorbed species, physical adsorption takes place. Otherwise, if the binding forces are strong and result in chemical bonds, then chemical adsorption or chemisorption occurs. In any case, one or more reactant substances become attached to the catalyst's surface;
4. Chemical Reaction. The reaction occurs on the catalyst's surface. It is desirable for this to be the most important step, the rate-controlling step of the chemical kinetics.
5. Desorption of the products. This process is the reverse of adsorption, where the products formed during the chemical reaction diffuse from the active sites of the catalyst;
6. Diffusion of the products from the interior of the pores to the external surface of the catalyst;
7. Diffusion of the products from the external surface of the catalyst back into the bulk fluid.

Stages 3, 4, and 5 are of a chemical nature and fundamentally depend on the nature of the catalyst used. Meanwhile, stages 1, 2, 6, and 7 are entirely of a physical nature.

To achieve this, two distinct mechanisms, Langmuir-Hinshelwood-Hougen-Watson [15–18] and Eley-Rideal [18,19] were employed, giving rise to 11 kinetic models. These models attempt to describe the combination of chemical and physical transformations that occur in the glycerol ketalization reaction with acetone, producing solketal and water, while utilizing heterogeneous catalysts of the rGO_H and rGO_E types.

Considering that there are no products at the beginning of the reaction, that is, $C_{C0} = C_{D0} = 0$, and knowing that, for a heterogeneous kinetics in a batch reactor, it holds that:

$$(-r_A) = \frac{C_{A_0}}{w_{cat}} \frac{dX_A}{dt} \quad \text{(Equation S11)}$$

When heterogeneous reactions are conducted under steady-state conditions, it is assumed that the steps of adsorption, chemical reaction, or desorption are equivalent.[13]

For this purpose, a reaction rate equation was obtained as a function of glycerol conversion (X_A) and time (min), multiplied by the mass of the catalyst used (w_{cat}) which, in this case, is 0.55 g, and the initial glycerol concentration (C_{A0} = 1.57 g mol^{-1}) for each of the 11 models obtained, with the assistance of Equation 17 and Table 8. And its rate is given as: [15,16,19]

$$(-r_A) = \frac{C_{A_0}}{w_{cat}}\frac{dX_A}{dt} = \frac{(kinetic\ factor)\times(driving\ force)}{(adsorption\ term)^n} \quad \text{(Equation S12)}$$

Table 8. Information about the type of rate-controlling step to assist in the assembly of heterogeneous kinetic models, including the kinetic factor, driving force, adsorption term, and the value of n (adsorption exponent). Adaptado de LHHW e ER. [15,16,19]

Controlling step	Kinetic factor	Driving force	Adsorption term	n
Adsorption of A	k_A	C_A-($C_C C_D$/KC_B)	(1+($K_A C_C C_D$/KC_B)+$K_B C_B$+$K_C C_C$+$K_D C_D$)^n	1
Adsorption of B	k_B	C_B-($C_C C_D$/KC_A)	(1+$K_A C_A$+($K_B C_C C_D$/KC_A)+$K_C C_C$+$K_D C_D$)^n	1
Dessorption of C	kcK	$C_A C_B$/C_D-(C_C/K)	(1+$K_A C_A$+$K_B C_B$+(K$K_C C_A C_B$/C_D)+$K_D C_D$)^n	1
Dessorption of D	k_DK	$C_A C_B$/C_C-(C_D/K)	(1+$K_A C_A$+$K_B C_B$+$K_C C_C$+(K$K_D C_A C_B$/C_C))^n	1
Only C desorbs	kcK	$C_A C_B$/C_D-(C_C/K)	(1+$K_A C_A$+(K$K_C C_A C_B$/C_D))^n	1
Only D desorbs	k_DK	$C_A C_B$/C_C-(C_D/K)	(1+ $K_B C_B$+(K$K_D C_A C_B$/C_C))^n	1
Reaction Surface	k$K_A K_B$	$C_A C_B$-($C_C C_D$/K)	(1+$K_A C_A$+$K_B C_B$+$K_C C_C$+$K_D C_D$)^n	2
Only A adsorbs	kK_A	$C_A C_B$-($C_C C_D$/K)	(1+$K_A C_A$+ $K_C C_C$)^n	2
Only B adsorbs	kK_B	$C_A C_B$-($C_C C_D$/K)	(1+$K_B C_B$+$K_D C_D$)^n	2

Mechanisms and conditions of the rate-controlling steps of the glycerol (A) ketalization reaction with acetone (B), producing solketal and water (D), for the construction of the models to be used:

1)Langmuir-Hinshelwood-Hougen-Watson Mechanism (LHHW) - This mechanism proposes that the glycerol ketalization reaction consists of three steps: in the first step, the adsorption of glycerol (A) and acetone (B) occurs at active sites; in the second step, a chemical reaction takes place between the reactants, glycerol (A) and acetone (B), on the surface resulting in the formation of Solketal (C) and water (D); in the final step, the desorption of Solketal (C) and water (D) occurs. [15,16]

Model 1: Reversible reaction, with no dissociation of reactants (A and B), controlling step: adsorption of glycerol (A);

$$\left(r_{ads,A}\right) = \frac{C_{A_0}}{w_{cat}} \times \frac{dX_A}{dt} = \frac{(k_{ads,A})\times\left(C_A - \left(\frac{C_C C_D}{KC_B}\right)\right)}{\left(1+\frac{K_A C_C C_D}{KC_B}+K_B C_B+K_C C_C+K_D C_D\right)} \quad \text{(Equation S13)}$$

Model 2: Reversible reaction, with no dissociation of reactants (A and B), controlling step: adsorption of acetone (B);

$$\left(r_{ads,B}\right) = \frac{C_{A_0}}{w_{cat}} \times \frac{dX_A}{dt} = \frac{(k_{ads,B})\times\left(C_B - \left(\frac{C_C C_D}{KC_A}\right)\right)}{\left(1+K_A C_A+\left(\frac{K_B C_C C_D}{KC_A}\right)+K_C C_C+K_D C_D\right)} \quad \text{(Equation S14)}$$

Model 3: Reversible reaction, with no dissociation of reactants (A and B), controlling step: chemical reaction between glycerol (A) and acetone (B), both adsorbed on the catalyst surface;

$$\left(r_{reaction}\right) = \frac{C_{A_0}}{w_{cat}} \times \frac{dX_A}{dt} = \frac{(k_{reaction} K_A K_B)\times\left(C_A C_B - \frac{C_C C_D}{K}\right)}{(1+K_A C_A+K_B C_B+K_C C_C+K_D C_D)^2} \quad \text{(Equation S15)}$$

Model 4: Reversible reaction, with no dissociation of reactants (A and B), controlling step: desorption of Solketal (C);

$$\left(r_{des,C}\right) = \frac{C_{A_0}}{w_{cat}} \times \frac{dX_A}{dt} = \frac{(k_{des,C}K)\times\left(\frac{C_A C_B}{C_D} - \frac{C_C}{K}\right)}{\left(1+K_A C_A + K_B C_B + \left(\frac{KK_C C_A C_B}{C_D}\right) + K_D C_D\right)} \quad \text{(Equation S16)}$$

Model 5: Reversible reaction, with no dissociation of reactants (A and B), controlling step: desorption of water (D);

$$\left(r_{des,D}\right) = \frac{C_{A_0}}{w_{cat}} \times \frac{dX_A}{dt} = \frac{(k_{des,D}K)\times\left(\frac{C_A C_B}{C_C} - \frac{C_D}{K}\right)}{\left(1+K_A C_A + K_B C_B + K_C C_C + \left(\frac{KK_D C_A C_B}{C_C}\right)\right)} \quad \text{(Equation S17)}$$

2)Eley-Rideal Mechanism - This mechanism suggests that only one of the reactants adsorbs onto the catalyst surface and reacts with the other reactant that remains in the liquid phase. This mechanism consists of three steps: in the first step, adsorption of one of the reactants, either glycerol (A) or acetone (B), occurs at active sites; in the second step, a chemical reaction takes place between the adsorbed acetone (B) or glycerol (A), with only one of the reactants adsorbed (A) or (B), while the other (B) or (A) remains in the liquid phase; finally, desorption of the product formed on the catalytic sites, Solketal (C) or water (D), occurs, with only one desorbing while the other is present in the liquid phase. [19]

Model 6: Reversible reaction, with no dissociation of reactants (A and B), controlling step: adsorption of glycerol (A);

$$\left(r_{ADS_A}\right) = \frac{C_{A_0}}{w_{cat}} \times \frac{dX_A}{dt} = \frac{(k_{ADS_A})\times\left(C_A - \left(\frac{C_C C_D}{KC_B}\right)\right)}{\left(1+\frac{K_A C_C C_D}{KC_B} + K_C C_C\right)} \quad \text{(Equation S18)}$$

Model 7: Reversible reaction, with no dissociation of reactants (A and B), controlling step: adsorption of acetone (B);

$$\left(r_{aADS_B}\right) = \frac{C_{A_0}}{w_{cat}} \times \frac{dX_A}{dt} = \frac{(k_{ADS_B})\times\left(C_B - \left(\frac{C_C C_D}{KC_A}\right)\right)}{\left(1+\left(\frac{K_B C_C C_D}{KC_A}\right) + K_D C_D\right)} \quad \text{(Equation S19)}$$

Model 8: Reversible reaction, with no dissociation of reactants (A and B), controlling step: chemical reaction between the adsorbed glycerol (A) on the catalyst surface (X) and the acetone (B) present in the liquid phase;

$$\left(r_{sr_{A.X}}\right) = \frac{C_{A_0}}{w_{cat}} \times \frac{dX_A}{dt} = \frac{(k_{sr_{A.X}}K_A)\times\left(C_A C_B - \frac{C_C C_D}{K}\right)}{(1+K_A C_A + K_C C_C)^2} \quad \text{(Equation S20)}$$

Model 9: Reversible reaction, with no dissociation of reactants (A and B), controlling step: chemical reaction between the adsorbed acetone (B) on the catalyst surface (X) and the glycerol (A) present in the liquid phase;

$$\left(r_{sr_{B.X}}\right) = \frac{C_{A_0}}{w_{cat}} \times \frac{dX_A}{dt} = \frac{(k_{sr_{B.X}}K_B)\times\left(C_A C_B - \frac{C_C C_D}{K}\right)}{(1+K_B C_B + K_D C_D)^2} \quad \text{(Equation S21)}$$

Model 10: Reversible reaction, with no dissociation of reactants (A and B), controlling step: desorption of Solketal (C);

$$\left(r_{DES_C}\right) = \frac{C_{A_0}}{w_{cat}} \times \frac{dX_A}{dt} = \frac{(k_{DES_C}K)\times\left(\frac{C_A C_B}{C_D} - \frac{C_C}{K}\right)}{\left(1+K_A C_A + \left(\frac{KK_C C_A C_B}{C_D}\right)\right)} \quad \text{(Equation S22)}$$

Model 11: Reversible reaction, with no dissociation of reactants (A and B), controlling step: desorption of water (D);

$$\left(r_{DES_D}\right) = \frac{C_{A_0}}{w_{cat}} \times \frac{dX_A}{dt} = \frac{(k_{DES_D}K)\times\left(\frac{C_A C_B}{C_C} - \frac{C_D}{K}\right)}{\left(1+K_B C_B + \left(\frac{KK_D C_A C_B}{C_C}\right)\right)} \quad \text{(Equation S23)}$$

Where M (dimensionless) is the ratio between the molar concentration of acetone C_{B0} and the molar concentration of glycerol C_{A0} (mol L^{-1}), $M = C_{B0}/C_{A0}$. The parameters K_A, K_B, K_C, and K_D (L mol^{-1}) are the adsorption equilibrium constants for the reactants A (glycerol), B (acetone), and the products C (Solketal) and D (water). K (dimensionless) is the thermodynamic equilibrium constant. The representations $k_{ads,A}$; $k_{ads,B}$; $k_{reaction}$; $k_{des,C}$; $k_{des,D}$; $k_{ADS,A}$; $k_{ADS,B}$; $k_{sr,A.X}$; $k_{sr,B.X}$; $k_{DES,C}$; $k_{DES,D}$ are related to the kinetic constant, k (g_{cat} L mol^{-1} min^{-1}), for each obtained model. While $r_{ads,A}$; $r_{ads,B}$; $r_{reaction}$; $r_{des,C}$; $r_{des,D}$; r_{ADSA}; r_{ADSB}; r_{ADSA}; $r_{sr,A.X}$; $r_{sr,B.X}$; $r_{DES,C}$; $r_{DES,D}$ corresponds to the reaction rate (mol L^{-1} g_{cat}^{-1} min^{-1}) for each obtained model.

References:

1. Maraschin, T.G.; Correa, R. da S.; Rodrigues, L.F.; Balzarettid, N.M.; Malmonge, J.A.; Galland, G.B.; de Souza Basso, N.R.; Basso, N.R. de S. Chitosan Nanocomposites with Graphene-Based Filler. *Mater. Res.* **2019**, *22*, 1–10, doi:10.1590/1980-5373-mr-2018-0829.
2. Sabzevari, M.; Cree, D.E.; Wilson, L.D. Graphene Oxide–Chitosan Composite Material for Treatment of a Model Dye Effluent. *ACS Omega* **2018**, *3*, 13045–13054, doi:10.1021/acsomega.8b01871.
3. Yang, X.; Tu, Y.; Li, L.; Shang, S.; Tao, X. Well-Dispersed Chitosan/Graphene Oxide Nanocomposites. *ACS Appl. Mater. Interfaces* **2010**, *2*, 1707–1713, doi:10.1021/am100222m.
4. Grande, C.D.; Mangadlao, J.; Fan, J.; De Leon, A.; Delgado-Ospina, J.; Rojas, J.G.; Rodrigues, D.F.; Advincula, R. Chitosan Cross-Linked Graphene Oxide Nanocomposite Films with Antimicrobial Activity for Application in Food Industry. *Macromol. Symp.* **2017**, *374*, 1600114, doi:10.1002/masy.201600114.
5. Zuo, P.-P.; Feng, H.-F.; Xu, Z.-Z.; Zhang, L.-F.; Zhang, Y.-L.; Xia, W.; Zhang, W.-Q. Fabrication of Biocompatible and Mechanically Reinforced Graphene Oxide-Chitosan Nanocomposite Films. *Chem. Cent. J.* **2013**, *7*, 39, doi:10.1186/1752-153X-7-39.
6. Kumar, A.S.K.; Jiang, S.-J. Chitosan-Functionalized Graphene Oxide: A Novel Adsorbent an Efficient Adsorption of Arsenic from Aqueous Solution. *J. Environ. Chem. Eng.* **2016**, *4*, 1698–1713, doi:10.1016/j.jece.2016.02.035.
7. Muda, M.S.; Kamari, A.; Bakar, S.A.; Yusoff, S.N.M.; Fatimah, I.; Phillip, E.; Din, S.M. Chitosan-Graphene Oxide Nanocomposites as Water-Solubilising Agents for Rotenone Pesticide. *J. Mol. Liq.* **2020**, *318*, 114066, doi:10.1016/j.molliq.2020.114066.
8. Han, D.; Yan, L.; Chen, W.; Li, W. Preparation of Chitosan/Graphene Oxide Composite Film with Enhanced Mechanical Strength in the Wet State. *Carbohydr. Polym.* **2011**, *83*, 653–658, doi:10.1016/j.carbpol.2010.08.038.
9. He, L.; Wang, H.; Xia, G.; Sun, J.; Song, R. Chitosan/Graphene Oxide Nanocomposite Films with Enhanced Interfacial Interaction and Their Electrochemical Applications. *Appl. Surf. Sci.* **2014**, *314*, 510–515, doi:10.1016/j.apsusc.2014.07.033.
10. Cobos, M.; González, B.; Fernández, M.D.J.; Fernández, M.D.J. Chitosan-Graphene Oxide Nanocomposites: Effect of Graphene Oxide Nanosheets and Glycerol Plasticizer on Thermal and Mechanical Properties. *J. Appl. Polym. Sci.* **2017**, *134*, 45092, doi:10.1002/app.45092.
11. Rossa, V.; Chenard Díaz, G.; Juvenal Muchave, G.; Alexandre Gomes Aranda, D.; Berenice Castellã Pergher, S. Production of Solketal Using Acid Zeolites as Catalysts. In *Glycerine Production and Transformation - An Innovative Platform for Sustainable Biorefinery and Energy*; IntechOpen, 2019; pp. 1–18.
12. Rossa, V.; Pessanha, Y. da S.P.; Díaz, G.C.; Câmara, L.D.T.; Pergher, S.B.C.; Aranda, D.A.G. Reaction Kinetic Study of Solketal Production from Glycerol Ketalization with Acetone. *Ind. Eng. Chem. Res.* **2017**, *56*, 479–488, doi:10.1021/acs.iecr.6b03581.
13. FOGLER, H.S. *Elementos de Engenharia Das Reações Químicas*; 3 rd.; Editora LTC: Rio de Janeiro, 2002;
14. Jr., C.G.H. *An Introduction to Chemical Enginnering Kinetics & Reactor Design*; John Wiley & Sons: New York;

15. Yang, K. H.; Hougen, O.A. Determination of Mechanism of Catalyzed Gaseous Reactions. *Chem. Eng. Prog.* **1950**, *46*, 146–157.
16. Hougen, O. A. and Watson, K.M. *Chemical Process Principles Part There Kinetics and Catalysis*; John Wiley: New York, 1959;
17. Chandra Shekara, B.M.; Ravindra Reddy, C.; Madhuranthakam, C.R.; Jai Prakash, B.S.; Bhat, Y.S. Kinetics of Esterification of Phenylacetic Acid with p -Cresol over H-β Zeolite Catalyst under Microwave Irradiation. *Ind. Eng. Chem. Res.* **2011**, *50*, 3829–3835, doi:10.1021/ie101134k.
18. Esteban, J.; Ladero, M.; García-Ochoa, F. Kinetic Modelling of the Solventless Synthesis of Solketal with a Sulphonic Ion Exchange Resin. *Chem. Eng. J.* **2015**, *269*, 194–202, doi:10.1016/j.cej.2015.01.107.
19. Eley, D.D.; Rideal, E.K. Parahydrogen Conversion on Tungsten. *Nature* **1940**, *146*, 401–402, doi:10.1038/146401d0.